International Journal of Chemical, Materials and Biomolecular Sciences
ISSN: 2415-6620
Vol:10, No:5, 2016

Applying Element Free Galerkin Method on Beam and Plate

Mahdad M'hamed, Belaidi Idir

***Abstract*—**This paper develops a meshless approach, called Element Free Galerkin (EFG) method, which is based on the weak form Moving Least Squares (MLS) of the partial differential governing equations and employs the interpolation to construct the meshless shape functions. The variation weak form is used in the EFG where the trial and test functions are approximated bye the MLS approximation. Since the shape functions constructed by this discretization have the weight function property based on the randomly distributed points, the essential boundary conditions can be implemented easily. The local weak form of the partial differential governing equations is obtained by the weighted residual method within the simple local quadrature domain. The spline function with high continuity is used as the weight function. The presently developed EFG method is a truly meshless method, as it does not require the mesh, either for the construction of the shape functions, or for the integration of the local weak form. Several numerical examples of two-dimensional static structural analysis are presented to illustrate the performance of the present EFG method. They show that the EFG method is highly efficient for the implementation and highly accurate for the computation. The present method is used to analyze the static deflection of beams and plate hole.

***Keywords*—**Numerical computation, element-free Galerkin, moving least squares, meshless methods.

I. Introduction

SINCE ten years, new digital alternatives to the finite element method (FEM) have been developed. They aim to avoid the difficulties related to the mesh by constructing a portion or all of the approximation by other approaches that the spatial discretization predetermined element. These techniques have brought certain ease in solving known problems to the FEM, like problem geometrical discontinuities (cracks, interface). Among these methods, we distinguish the mesh free methods. The so-called meshless methods construct approximations from a set of nodal data without the need for any (finite-element) a priori connectivity information between the nodes [1]. In general, a meshless method uses a local interpolation or approximation to represent the trial function with the values (or the fictitious values) of the unknown variable at some randomly located nodes [2], [3].

Compared with FEM, the meshless methods can easily handle large deformation and strongly nonlinear problems, since the connectivity among the nodes is generated as a portion of computation and it can change with time. The method meshless is less susceptible to mesh distortion difficulties than FEM.

In meshless methods, the influence domains may and must overlap each other, in opposition to the no-overlap rule between elements in the FEM. In the meshless methods, the nodes can be arbitrary distributed, once the field functions are approximated within an influence domain rather than an element. The meshless methods can solve complex problems without generating any mesh. The method should also correctly handle the governing differential equations with the appropriate boundary conditions, Fig. 1. The numerical integration is performed by the Gauss quadrature with the Gauss points, and then the results are interpolated at the field nodes. This makes a further approximation of the values of function at the field nodes [4].

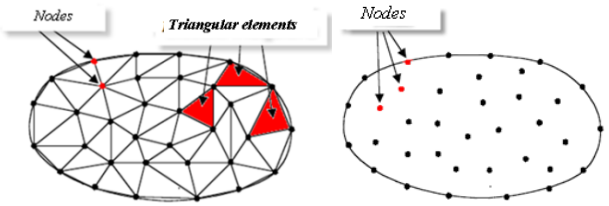

(a) (b)

Fig. 1 Numerical computations of (a) FEM, (b) EFG

Meshless methods construct approximations entirely in terms of nodes. The approximation function is an essential feature of the method. A weight function, which plays an important role in the performance of the methods, is used in all varieties of meshless methods. The compact support of weight functions, also called the domain of influence of a node, gives a local character to the meshless methods. The weight function is nonzero in the domain of support and zero outside of the domain of support. The most commonly used supports are discs and rectangles [5].

Many of meshless methods have been developed, such as the diffuse element method (DEM), EFG method, the finite point method (FPM), meshless local Petrov Galerkin (MLPG) method, the multi-scale reproducting kernel particle (MRKP) method, wavelet particle method (WPM), the radial basis functions (RBF) method, the meshless finite element method (MFEM) [5], [6]. The purpose of the shape function is to approximate the field functions using their values at sampling nodes in the analysis domain. (MLS) approximation has been used for constructing the shape function in EFG [7].

Belytschko et al. [8] used MLS interpolants to construct the trial and test functions for the variational principle (weak

Mahdad M'hamed and Professeur Belaidi Idir, M'hamed Bougara are with the University of Boumerdes, Avenue de l'independence Boumerdes, Algeria (phone: (0213)26 40 1479 / 02; fax: (0213)26 40 1478); e-mail: mahdadm@yahoo.fr).

form) and weight functions. In contradistinction to DEM, they introduced certain key differences in the implementation to improve the accuracy. Chen et al. [9] showed that for convergence, an integration constraint (IC) is introduced as a necessary condition for a linear exactness in the mesh-free Galerkin approximation.

Among the meshfree methods, EFG meshfree method is one of the best known and most robust one; it is based on the resolution of the low form of partial differential equations by a method Galerkin [10]. The approximation of the displacement field that is built to be introduced into the weak form does not require a mesh, but only a set of points distributed over the field. EFGM offers several advantages. First, it eliminates the creation of elements in the classical FEM. Second, the postprocessing of strains and stresses is required in the FEM to obtain smooth field plots, whereas no such postprocessing is required in the EFGM as these fields are already smooth. Third, the performance of the EFGM seems to be independent of nodal point arrangement. Also, an incompressible material can be treated by EFGM without any modifications.

Zhang et. al [11] used moving least-square technique to construct shape function in the EFGM at present, but sometimes the algebra equations system obtained from the moving least-square approximation is ill-conditioned and the shape function needs large quantity of inverse operation. Soparat et al. [12] extended the EFGM to include nonlinear behavior of cracks in 2D concrete. The paper presents a numerical simulation of mechanical structures, based on EFG.

In this work, the performance of distinct meshless EFG techniques written in Matlab is compared with FEM method implemented in ANSYS for assessing the convergence, in the case of digital simulation of the static behavior of beams, plate with a central and elliptic hole.

II. Meshless Method and MLS Approximation

EFGM was developed by Belytschko et al. [9] based on Diffuse Elements Method developed by Nayroles et al. [13]. EFG method has some major features;

1. MLS approximation is implemented to construct the shape functions.
2. Galerkin Weak form with constraints to apply the essential Boundary conditions is used to develop the discrete equation system equations.
3. EFG is a pseudo mesh free method as it requires background cells for performing numerical Integrations to construct the system matrices

A. MLS Approximation

Following is the procedure for constructing shape functions for mesh free methods using MLS approximation [14].

Let *u(x)* the function of the field variable in the domain Ω, the approximation of *u(x)* is denoted by $u^h(x)$.

In MLS, we approximate the field function in the form of series representation as:

$$u^h(x) = \sum_{j=1}^{m} p_j(x) a_j(x) = p^T a(x) \tag{1}$$

where, m is the number of monomials (polynomial basis) *a(x)* is the vector of coefficients given by

$$a^T(x) = \{a_0(x) a_1(x) \ldots\ldots\ldots\ldots a_{m-1}(x) a_m(x)\} \tag{2}$$

We should note that *a(x)* is an arbitrary function of x. A functional of weighted residual is then created using the approximated values of the values of the field function and the nodal parameters $u_I = u(x_I)$.

$$J = \sum_{i=1}^{n} w(x - x_1)\left[u^h(x - x_1)(x_1)\right]^2 \tag{3}$$

$$J = \sum_{i=1}^{n} w(x - x_1)\left[p^T(x_1) a(x) - u_1\right]^2 \tag{4}$$

where $w(x-x_I)$ is a weight function. Weight functions play their role effectively when sufficient nodes are used.

$$\frac{\partial J}{\partial a} = 0 \tag{5}$$

This gives us the following expression of the coefficient vector:

$$a(x) = A^{-1}(x) B(x) u_s \tag{6}$$

where A is called the MLS moment matrix given by

$$A(x) = \sum_{i=1}^{m} w(x) p^T(x_1)\, p(x_1) \tag{7}$$

where $w(x) = w(x-x_I)$ and B(x) has the form

$$u^h(x) = \sum_{i=1}^{n} \varphi(x) u_1 \tag{8}$$

where φ(x) is the MLS shape function defined by

$$\varphi(x) = \sum_{i=1}^{m} p_i(x) A^{-1}(x) B(x)\, j_i u_i = p^T A^{-1} B_1 \tag{9}$$

This leads us to another important thing about applying the essential boundary conditions on the weak form since we cannot apply boundary conditions directly to u_I. Therefore, we use Lagrange multipliers to enforce the essential boundary condition.

B. Support Domain and Weight Function

Works of Bui [15] confirm that the results vary somewhat from the chosen weight function. For the case of two dimensions, the weight function is applied to a circular area (where r is the radius of the sphere of influence) and rectangular. There is no difference if a circular or rectangular support domain is used in the EFG method. Weight functions are functions that are assigned a space of influence (Wi) for

each point at which it is associated. The area of influence must be non-zero and of course included in the domain W.

A weight function needs properties as:

- Compact support, i.e. zero outside the support domain.
- The value of all points in the support domain is positive.
- The value of its maximum at the current point and decrease when moving outwards.

There are many kinds of function satisfying for these properties. In this paper, we used the quadratic spine function as:

$$w(d_I)=\begin{cases}1-6\left(\frac{d_I}{d_{mI}}\right)^2+8\left(\frac{d_I}{d_{mI}}\right)^3-3\left(\frac{d_I}{d_{mI}}\right)^2 & d_I \le d_{\mathrm{Im}}\\ 0 & d_I \le d_{\mathrm{Im}}\end{cases}$$

C. EFG Formulation

Partial differential equations and boundary conditions of the system (2D problem) can be written as

$$L^T\sigma+b=0 \tag{10}$$

The boundary conditions are given as:

$$u=\bar{u} \quad on \quad \Gamma_t \tag{11}$$

where L is the divergence operator.

$$L=\begin{bmatrix}\partial/\partial x & 0\\ 0 & \partial/\partial y\\ \partial/\partial y & \partial/\partial x\end{bmatrix} \tag{12}$$

where L is a differential operator matrix dependent on the strain types, we arrive at:

$$\int_\Omega \delta(Lu)^T(cLu)d\Omega-\int_\Omega \delta u^T b\,d\Omega-\int_{\Gamma_t}\delta u^T\bar{t}\,d\Gamma-\int_{\Gamma_u}\delta\lambda^T(u-\bar{u})\,d\Gamma-\int_{\Gamma_u}\delta u^T\lambda\,d\Gamma=0 \tag{13}$$

Equation (13) then becomes:

$$\delta U^T\left[KU-F\right]+\delta\Lambda^T(G^TU-Q)+\delta U^TG\Lambda=0$$
$$\delta U^T\left[KU+G\Lambda-F\right]+\delta\Lambda^T(G^TU-Q)=0$$

This can be written as:

$$\begin{cases}KU+G\Lambda-F=0\\ G^TU-Q=0\end{cases} \tag{14}$$

III. Numerical Results and Discussions

As a first challenge to understand the EFG method, a program for linear static with MATLAB was implemented. This solution was made by Timoshenko and Goodier [16]. Consider a beam, as shown in Fig. 2, with length L and height D subjected to a parabolic traction at the free end. The parameters of the beam are taken as E = 3.10^7, m = 0.3, D = 12, L = 48, and P = 1000. The beam has a unit thickness and a plane stress problem is considered.

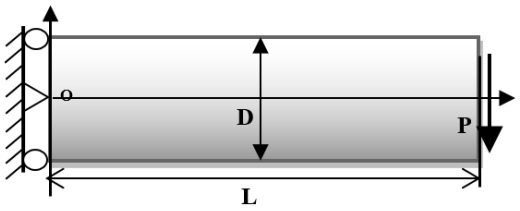

Fig. 2 A cantilever beam subjected to a parabolic traction at the free end

The traction vector at the free end (x=48) are parabolic and given by

$$t_y=-\frac{P}{2I}\left(\frac{D^2}{4}-y^2\right) \tag{15}$$

The moment of inertia for a rectangular surface with unit thickness is

$$I=\frac{D^3}{12} \tag{16}$$

The displacement in the x direction is given by

$$u(x,y)=-\frac{Py}{6EI}\left[(6L-3x)x+(2+\nu)\left(y^2-\frac{D^2}{4}\right)\right] \tag{17}$$

The displacement in the y direction is given by

$$v(x,y)=\frac{P}{6EI}\left[3\nu y^2(L-x)+(4+5\nu)\frac{D^2x}{4}+(3L-x)x^2\right] \tag{18}$$

Fig. 3 shows the model Meshless of the deformed and undeformed beam.

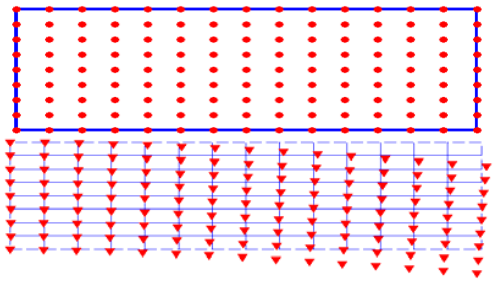

Fig. 3 Nodal discretization with beam

The results of the displacement obtained by the EFG and the analytical model for the beam are given in Fig. 4.

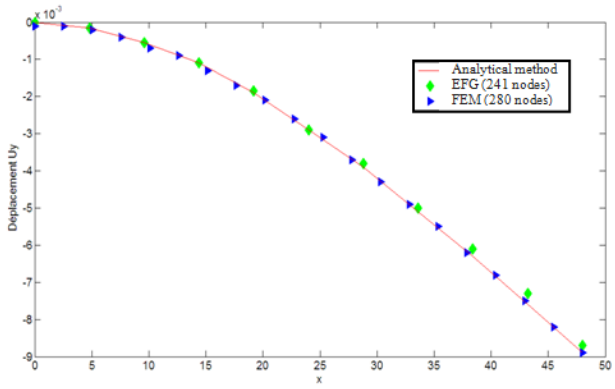

Fig. 4 Vertical displacement Uy of the beam to the central axis (y = 0) obtained by the EFG method and the analytical model

The results of the numerical solution obtained with the EFG method can be considered satisfactory and close to the analytics solution. The relative errors of displacements *ux* exact and *uy* computed (EFG) are considered for in Table I.

TABLE I
COMPARISON OF THE EXACT SOLUTION AND THE COMPUTED SOLUTION

Nodes	u_y exact	u_y EFG	Relative error (%)
7*5	- 0.0089	- 0.0083	6.74
11*5	- 0.0089	- 0.0087	2.24
15*9	- 0.0089	- 0.0088	1.12
20*9	- 0.0089	- 0.0088	1.12

Consider an infinite plate with a central hole: $x^2+y^2 \leq a^2$ (a is the radius of the hole), which is subjected to a unit uniform tension ($\sigma = 1$) in x direction at infinity (Fig. 5).

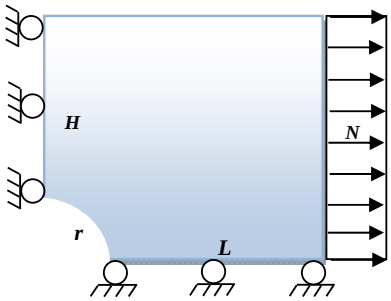

Fig. 5 The infinite plate with a central hole

Due to the symmetry, only quarter of the plate is modeled as shown in Fig. 4. For this plane strain problem, the material properties are taken as E = 1000 and $\nu = 0.3$. Symmetry conditions are imposed on the left and bottom edges, and the inner boundary at $x^2+y^2 \leq a^2$ is traction free.

Timoshenko and Goodier [16] detail the analytical model of the stresses on an infinite plate with a hole in the center. It is subject to normal traction (Nx) in the direction ox. The stress distributions in the perforated plate (and) is described by:

$$\sigma_{xx} = N_x\left[1-\frac{R^2}{r^2}\left(\frac{3}{2}\cos(2\theta)+\cos(4\theta)\right)+\frac{3}{2}\frac{R^2}{r^2}\cos(4\theta)\right] \quad (19)$$

$$\sigma_{yy} = N_x\left[-\frac{R^2}{r^2}\left(\frac{3}{2}\cos(2\theta)-\cos(4\theta)\right)-\frac{3}{2}\frac{R^4}{r^4}\cos(4\theta)\right] \quad (20)$$

$$\sigma_{xy} = N_x\left[1-\frac{R^2}{r^2}\left(\frac{3}{2}\sin(2\theta)+\sin(4\theta)\right)+\frac{3}{2}\frac{R^4}{r^4}\sin(4\theta)\right] \quad (21)$$

The simulation with the FEM with ANSYS software uses PLANE42 elastic elements which are formed by 4 nodes and 2 d.d.l [17]. Modeling procedure with EFG uses the generation of points of ANSYS in its procedures for an even distribution points (Fig. 7).

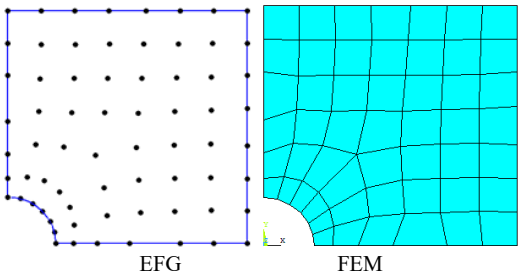

(a) 67regular nodes

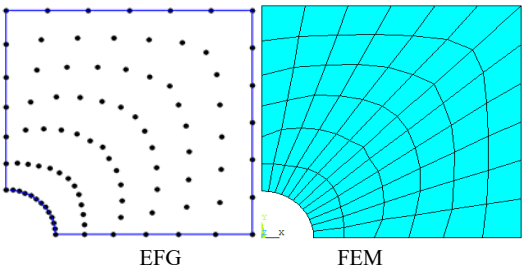

(b) 91regular nodes

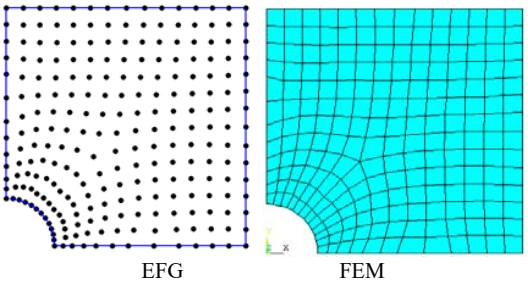

(c) 241 irregular nodes

Fig. 6 Distribution in the plate with a central holefor FEM and EFG methods

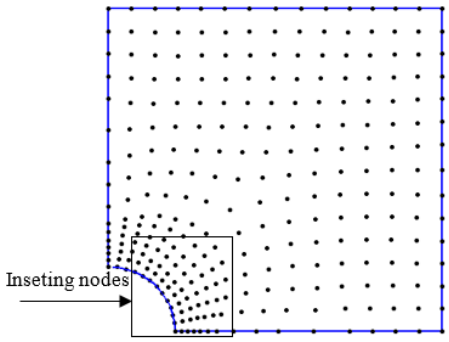

Fig. 7 Irregularly distribution 280 nodes EFG Method

In Fig. 7, 280 nodes are arranged irregularly in both h and r directions.

The meshfree code has successfully simulated the displacement and stress in the plate with a central hole.

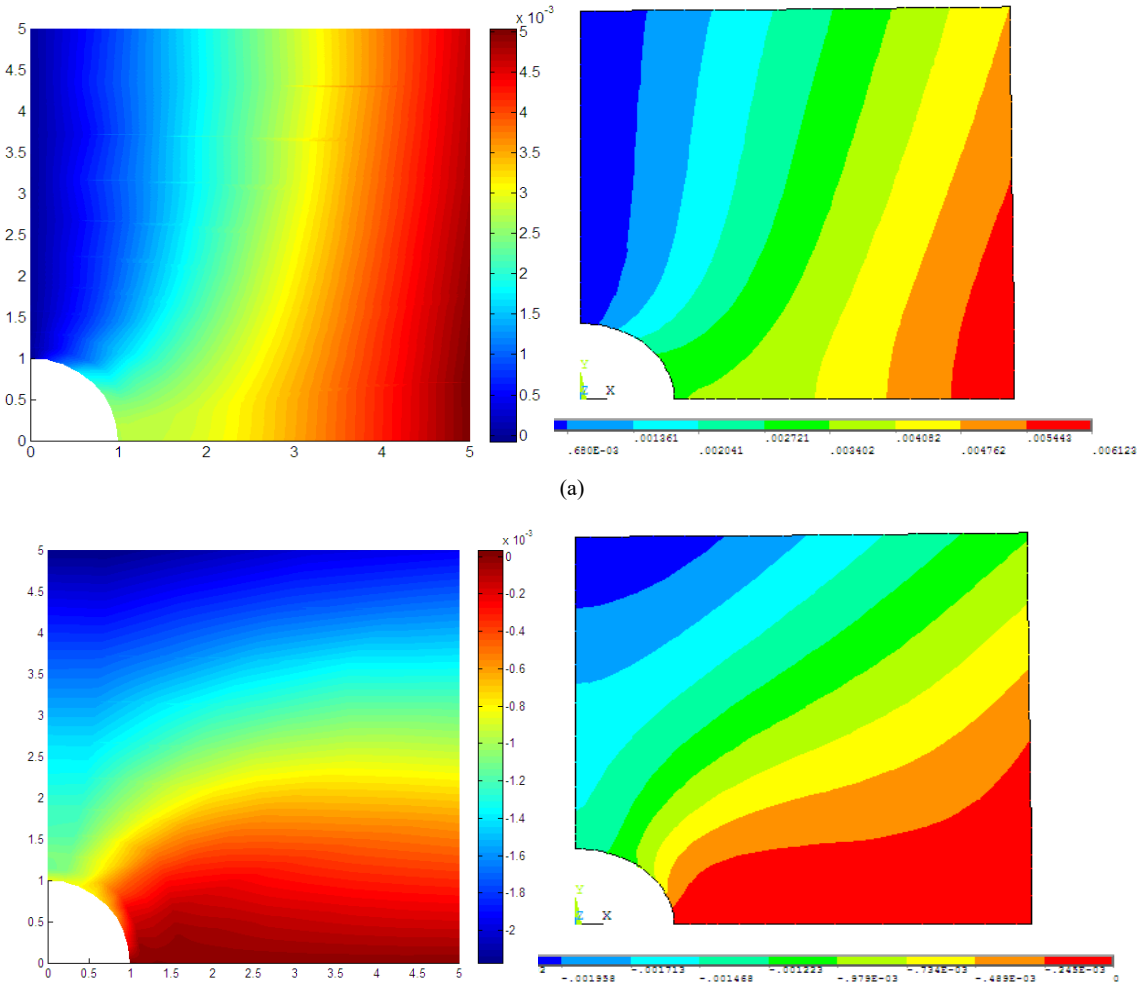

Fig. 8 Displacement (*ux, uy*) along x = 0 for the plate with a central hole, (a) displacement *ux,* (b) displacement *(uy)*

Fig. 9 shows the distribution of stress along x=0 for the plate. This application illustrates the benefits of EFG method to a distribution of stress in a square plate having a crack (hole).

The variations between the analytical results and those obtained by the two numerical methods are also shown in Fig. 10.

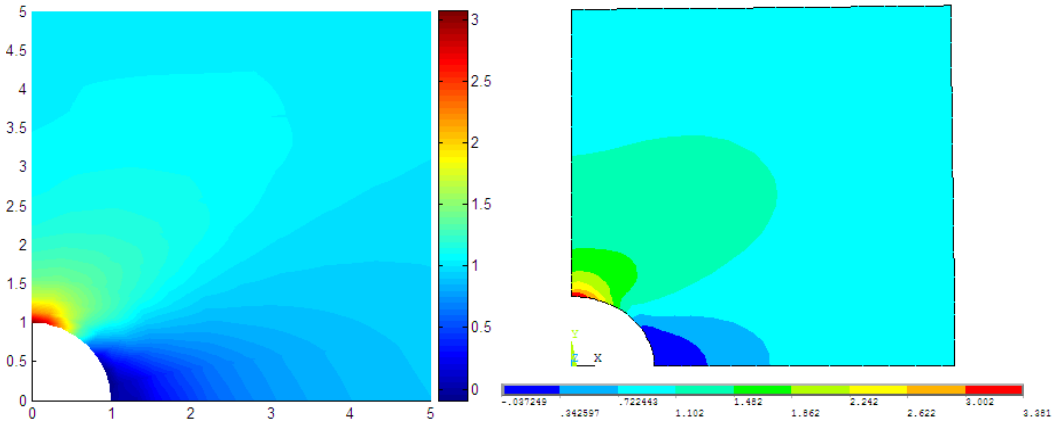

(a)

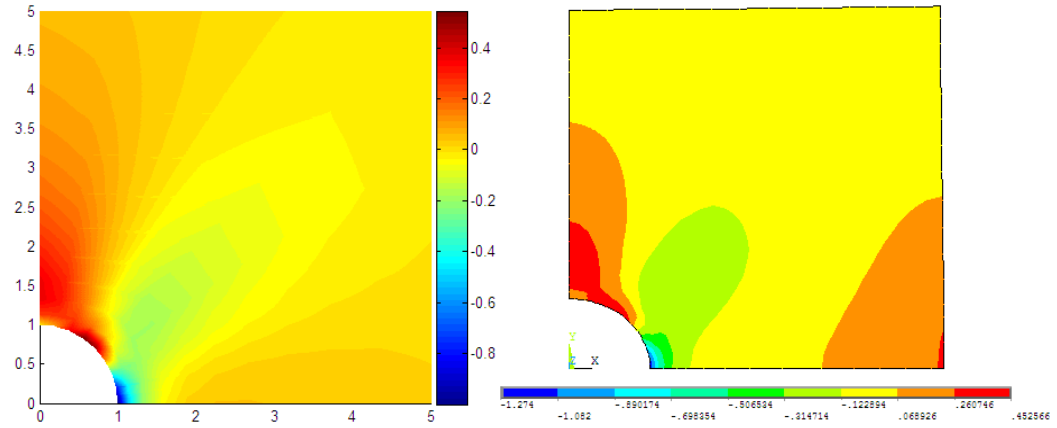

(b)

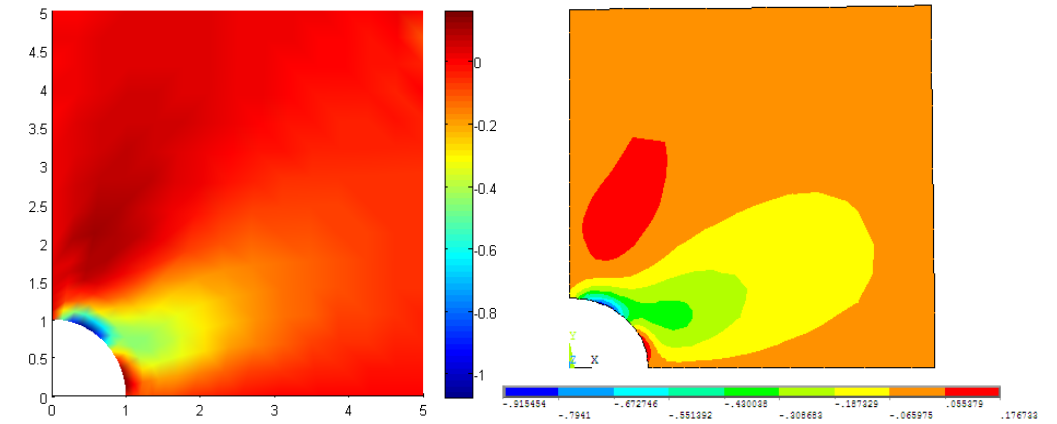

(c)

EFG FEM

Fig. 9 Distribution stress along x = 0 for the plate with a central hole, (a) Distribution Stress σ_{xx}, (b) Distribution stress σ_{yy}, (c) Distribution stress σ_{xy}

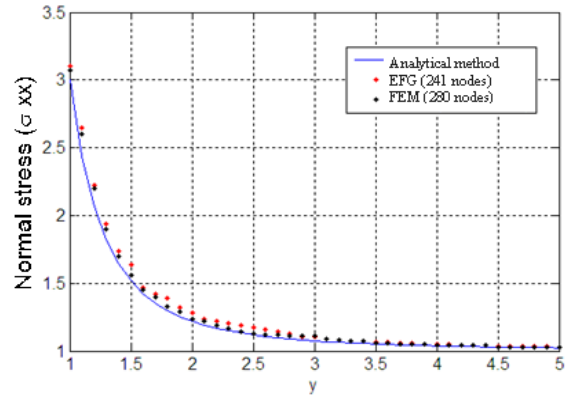

(a)

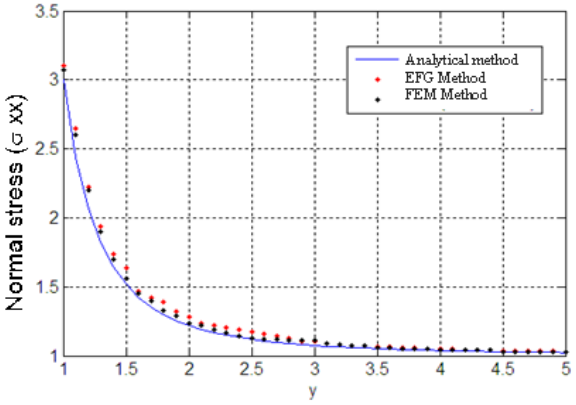

(b)

Fig. 10 The normal stress σ_{xx} along x = 0 for the plate with a central hole

We note that the superposition of values related stress curves obtained by numerical methods EFG and MEF one hand, and the confrontation with the analytical solution on the other hand, produced almost the same values, which convergence the method EFG implemented for modeling square plates in the presence of failure. The calculation time is different for the two modeling techniques due to the integration features and size of the system of equations solved by the two numerical methods. It should be mentioned here that for this problem, the method meshfree EFG uses less computational cost than the method FEM, essentially when apply the meshfree method in a very small region.

Fig. 10 presents the comparison of computed results with the exact solution for the stress σ_{xx} along x = 0. This comparison shows that the numerical solutions of 91-node and 241-node as shown in Fig. 10 (a) are all satisfactory. Furthermore, the results of 241 nodes are more accurate than that of 91 nodes. Fig. 10 (b) shows the numerical results of regularly and irregularly distributed 280 nodes. Again, it can be found that the results in these two cases agreed well with the exact solution.

The energy norm can comprehensively reflect the accuracy of strain and stress. The energy norm is defined as:

$$\|\varepsilon\| = \left\{ \frac{1}{2} \int_{\Omega} \left(\varepsilon^{Num} - \varepsilon^{Exact} \right)^T D \left(\varepsilon^{Num} - \varepsilon^{Exact} \right) d\Omega \right\}^{\frac{1}{2}} \quad (22)$$

The results of the convergence rates are shown in Fig. 11. A similar comparison with [8] shows comparable results for the relative error in energy, but less accurate results when comparing the relative error in displacements *log10ru*.

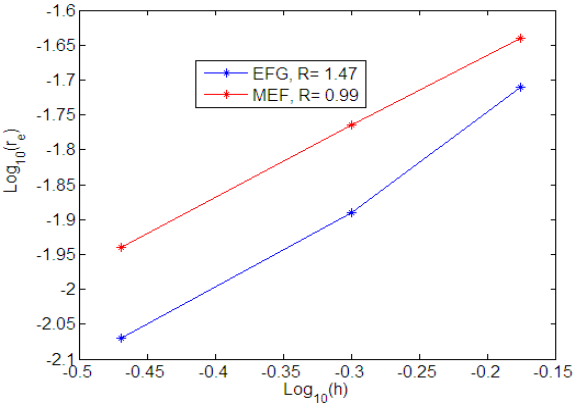

Fig. 11 The convergence study for the plate with circular hole

For complex mechanical parts geometries (Fig. 12), the presence of a spherical or ellipsoidal inclusion in the square dimension of plate is similar to the previous problem, with an elliptical crack.

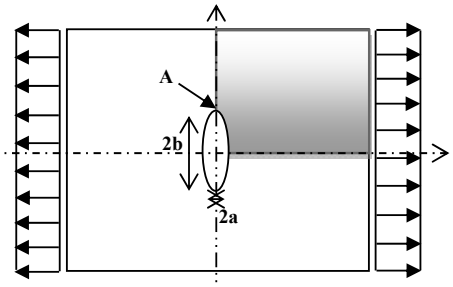

Fig. 12 The infinite plate with a central elliptic geometry of crack

The maximum stress is located at the crack tip (point A) of the plate with an elliptic geometry of crack. The stress distributions in the perforated plate are described by:

$$\sigma_A = \sigma \left(1 + \frac{2b}{a} \right) \quad (23)$$

The simulation with the FEM with ANSYS model uses PLANE42 elastic elements which are formed by 4 nodes and 2 d.d.l. All the problems have been simulated by EFG codes (algorithms) writing in MATLAB.

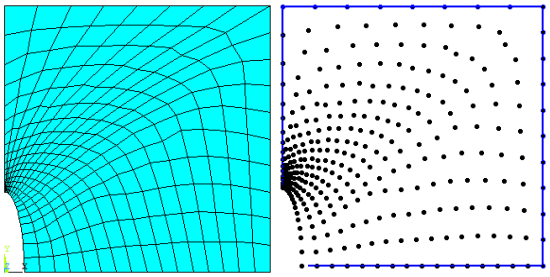

Fig. 13 Nodal distribution in the plate with an elliptic geometry of crack for FEM and EFG methods (333 nodes)

Fig. 14 shows the nodes distribution with EFG method adapted along the plate.

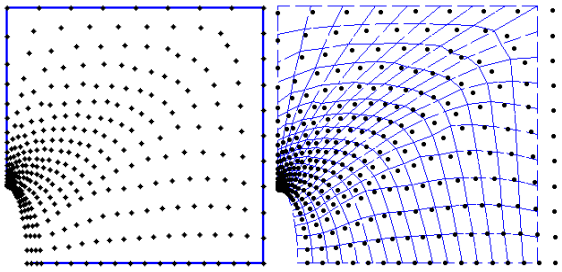

Fig. 14 Irregularly distribution 361 with nodes EFG Method

The distributions of horizontal displacements in the elliptical plate, with the two simulated numerical methods, are shown in Fig. 15.

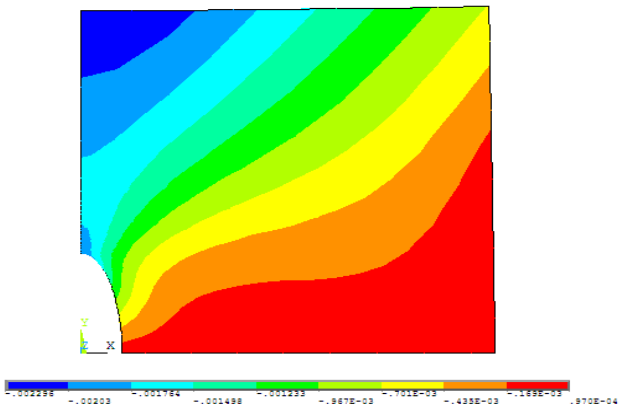

(a)

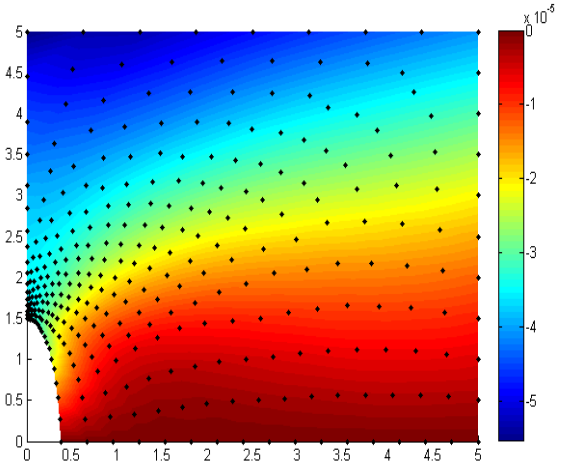

(b)

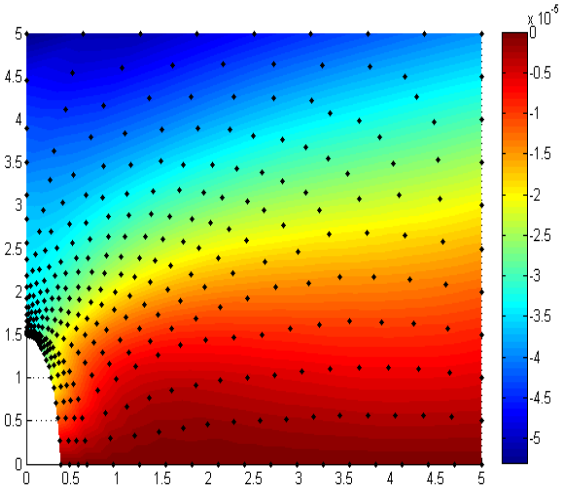

(c)

Fig. 15 Displacement (*ux*) along x = 0 for the plate, (a) *ux* FEM, (b) *ux* EFG, (c) *ux* EFG adapted

The Meshfree code has successfully simulated the displacement and stress in the plate with a central elliptic geometry of crack. The results of the numerical solution obtained with the EFG method can be considered satisfactory and that are close to the Analytics solution.

IV. Conclusion

A new meshless approach, called EFG method, has been developed for problems of linear elasticity. In the present method, the interpolation technique is employed to construct the shape functions with the weight function property by using the scattered points. This property of the shape functions makes it easy to impose the essential boundary conditions.

The numerical results demonstrate that the EFG method presented in this paper is easy to implement, and the computational accuracy is good for the displacements and stresses. The convergence study shows that the presently

developed EFG method possesses good convergence for the problem considered.

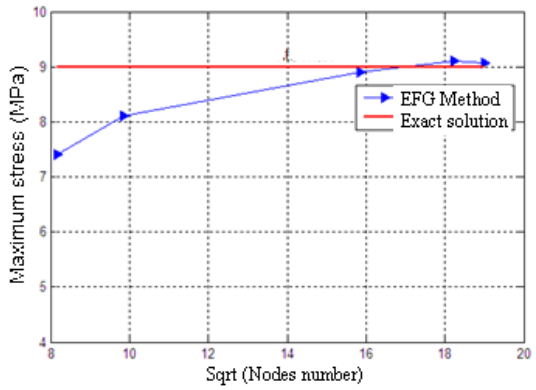

Fig. 16 The normal stress σ_{xx} along x= 0 for the plate with a central elliptic geometry of crack

ACKNOWLEDGMENT

The research subject is proposed by Professor Idir Belaidi of EMI laboratory (Modeling and simulation in mechanical engineering) of Boumerdes University.

REFERENCES

[1] P. Metsis, N. Lantzounis, M. Papadrakakis. A new hierarchical partition of unity formulation of EFG meshless methods. Computer Methods in Applied Mechanics and Engineering, 2015, vol 283, pp 782-805.
[2] T.R. Chandrupatla and A.D. Belegundu, "Introduction to Finite Element in Engineering" 2002, Ed. 3rd.
[3] C.V. Le, H. Askes, M. Gilbert, Adaptive element-free Galerkin method applied to the limit analysis of plates, Comput. Methods Appl. Mech. Engrg. 199 (37–40) (2010) 2487–2496.
[4] Zhu T and Atluri SN, A modified collocation a penalty formulation for enforcing the essential boundary conditions in the element free Galerkin method. Comput. Mech., 21, pp 211-222. 2007.
[5] Belytschko T, Krongauz Y, Organ D, Fleming M, Krysl P. method: an overview and recent developments. Computer Methods in Applied Mechanics and Engineering 1996; 13.
[6] Atluri SN, Zhu T (2000) The meshless local Petrov–Galerkin (MLPG) approach for solving problems in elasto-statics. Comput. Mech. 25: pp169–179.
[7] Liu W. K. Li S, Belytschko T, Moving least square reproducing kernel method (I) methodology and convergence. Comput. Meth. Eng. 1997.
[8] T. Belytschko, Y.Y. Lu, L. Gu, "Element-free Galerkin methods". International Journal of Numerical Methods in Engineering, 1994, vol. 37, pp. 229-256.
[9] J. S. Chen, C. T. Wu, S. Yoon, Y. You, "A Stabilized conforming nodal integration for galerkin mesh free methods", International Journal of Numerical Methods in Engineering, 2001, vol. 50, pp. 435-466.
[10] Hua Li, Shantanu S. Mulay. Meshless Method and their numerical proprieties. CRC Press, Taylor and Francis Group, 2013.
[11] Y. Zhang, M. Xia, Y. Zhai, "Analyzing Plane-plate Bending with EFGM", 2009, Journal of Mathematics Research, vol.-1, no-1.
[12] P. Soparat, P. Nanakorn," Analysis of crack growth in concrete by the element freegalerkin method", pp. 42-46.
[13] Nayroles B., Touzot G., Villon P. Generalizing the finite element method: diffuse approximation and diffuse elements. Computational mechanics, 1992, 10: 307–318.
[14] Dolbow J, Belytschko T., An Introduction to Programming the Meshless Element Free Galerkin Method, Archives of Computational Methods in Engineering, 5(3), 207-241 (1998).
[15] Bui Manh Tuan, Chen Yun Fei. Analysis and prediction of crack propagation in plates by the enriched free Galerkin method. International Journal of Mechanical Engineering and Applications, 2014; 2(6): 78-86.
[16] Timoshenko SP, Goodier JN. Theory of elasticity. 3rd ed. New York: McGraw-hill; 1970.
[17] ANSYS User's Guide, Revision 12.0 Tutorials, Swanson Analysis System, 2014.